Integrating photonic and microfluidic structures on a device fabricated using proton beam writing

A. A. Bettiol^a, E.J. Teo^b, C.N.B. Udalagama^a, S. Venugopal Rao,^{c} J.A. van Kan^a, P. G. Shao^a and F. Watt^a

^{a}Centre for Ion Beam Applications, Department of Physics, National University of Singapore, 2 Science Dr 3 Singapore 117542

^{b}Department of Materials Science and Engineering, National University of Singapore, 9 Engineering Dr 1, Singapore 117576

^{c}Department of Physics, Indian Institute of Technology Guwahati, Guwahati 781039, Assam, India

ABSTRACT

Proton beam writing is a lithographic technique that can be used to fabricate microstructures in a variety of materials including PMMA, SU-8 and Foturan^{TM}. The technique utilizes a highly focused mega-electron volt beam of protons to direct write latent images into a material which are subsequently developed to form structures. Furthermore, the energetic protons can also be used to modify the refractive index of the material at a precise depth by using the end of range damage. In this paper we apply the proton beam writing technique to the fabrication of a lab-on-a-chip device that integrates buried waveguides with microfluidic channels. We have chosen to use Foturan^{TM} photostructurable glass for the device because both direct patterning and refractive index modification is possible with MeV protons.

Keywords: Keywords: proton beam writing, glass, waveguides, microfluidics

1. INTRODUCTION

Lab-on-a-chip devices for biological analysis that rely on optical techniques for high sensitivity detection are sometimes known as biophotonic chips.[1] Biophotonic chips typically require optical elements in order to provide both a source of excitation, for example a laser to excite florescence, and to efficiently collect the emerging light for analysis. Both excitation and detection can usually be achieved in a laboratory setup using an optical microscope with a high numerical aperture objective. For applications that require low cost solutions, disposable polymeric or glass lab-on-a-chip devices are necessary. Disposable biophotonic lab-on-a-chip devices may include any number of microfluidic channels along with integrated waveguides or microlenses depending on the application. The function of the integrated optics is to direct light to a specific region of the chip, or for efficient light collection. These microoptical elements have the added advantage that optical alignment to the analysis region of the chip is achieved during the fabrication process.

Several methods are currently being employed for the fabrication of biophotonic chips with integrated waveguides. Waveguides can be integrated onto a chip using ion exchange or laser direct writing.[2,3] Laser direct writing has the additional advantage that it also can be used to fabricate buried microfluidic channels in the glass or polymer sample.[4] Typically these fabrication techniques can be combined with other conventional lithographic processes in order to fabricate different parts of the chip.

In this paper we present an alternative method for the fabrication of an integrated biophotonic chip known as Proton Beam Writing (PBW).[5] PBW is a new emerging lithographic technique that uses a focused beam of

---

mega electron volt (MeV) protons to scan across a sample allowing for predetermined patterns to be directly fabricated in various materials. Being a direct write technique, PBW is well suited to rapid prototyping tasks because no mask is required for fabrication. We utilize the PBW technique to fabricate both the microfluidic channels and the integrated waveguides of the biophotonic chip.

To demonstrate the use of PBW for biophotonic chip fabrication, Foturan^{TM} glass is used as the biochip material. Foturan^{TM} is a photosensitive glass (Manufactured by Schott Mikroglass) that can be directly patterned using conventional UV lithography,[6] femtosecond lasers[7–9] and MeV protons.[10–12] Unlike other glasses that require masking in order to allow for the formation of patterns, irradiated regions of Foturan^{TM} have a 20 times increase in etch rate after heat treatment. The ability to directly form microstructures in this glass along with its resistance to high temperature and corrosion has made it a particularly attractive platform for microfluidic applications such as microelectrochemical reactors.[13, 14] Furthermore, its high transparency and the ability to modify the refractive index of this glass makes it equally attractive for the fabrication of micro optical components such as waveguides[15] and gratings.[16]

2. EXPERIMENT

Commercial Foturan^{TM} samples were cut and mechano-chemically polished along the edges to achieve an optical finish. The final polished samples were approximately $15\times8\times2$ mm in size. Microchannels and waveguides were fabricated using the proton beam writing facility at the National University of Singapore. A schematic diagram of the fabrication steps for producing a microfluidic chip with integrated waveguides is shown in figure 1.
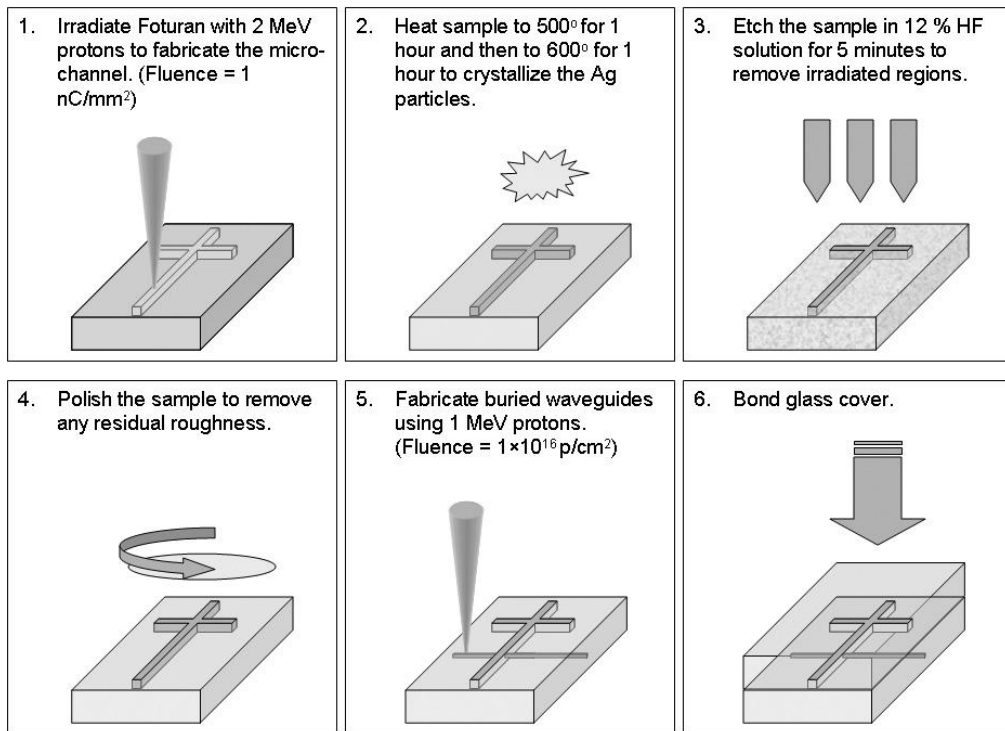

Figure 1. Schematic diagram showing the processing steps involved for fabricating a combined microchannel and optical waveguide device using proton beam writing.

2.1. Microchannel fabrication

Two microchannels in a cross configuration, 6 mm and 8 mm in length, were fabricated in the Foturan^{TM} sample using PBW. A beam of 2 MeV protons focused down to approximately 1-2 μm was magnetically scanned over a width of 40 μm perpendicular to a constant linear motion provided by an EXFO Burleigh inchworm stage. The stage speed used for the scan was 4 μm/s and the proton fluence delivered to the sample was 2 nC/mm^2. This irradiation process leads to the formation of a latent image in the Foturan^{TM} that can be later developed to form microchannels. An overview of the sample is shown in figure 2a.

Post irradiation, the sample is slowly heated to 500°C at a rate of 2° per minute. The sample is then held at this temperature for one hour before the temperature is raised to 600°C at a rate of 2° per minute. The sample is then held to 600°C for a further hour before being allowed to cool to room temperature. This heat treatment process results in the formation of lithium-metasilicate (Li$_2$SiO$_3$) crystallites in the irradiated region. Lithium-metasilicate is typically brown in color making it easily visible. An optical image of the "cross" region of the sample after heat treatment is shown in figure 2b.

To form the microchannel, the heat treated sample was etched in a 12% hydrofluoric acid solution for 5 minutes and then washed and sonicated in iso-propyl alcohol for a few minutes. Preferential etching of the irradiated regions occurs because the lithium-metasilicate is etched at a rate that is approximately 20 times higher than the SiO$_2$ in the unirradiated regions. Figure 2c shows an optical image of the microchannel after etching.
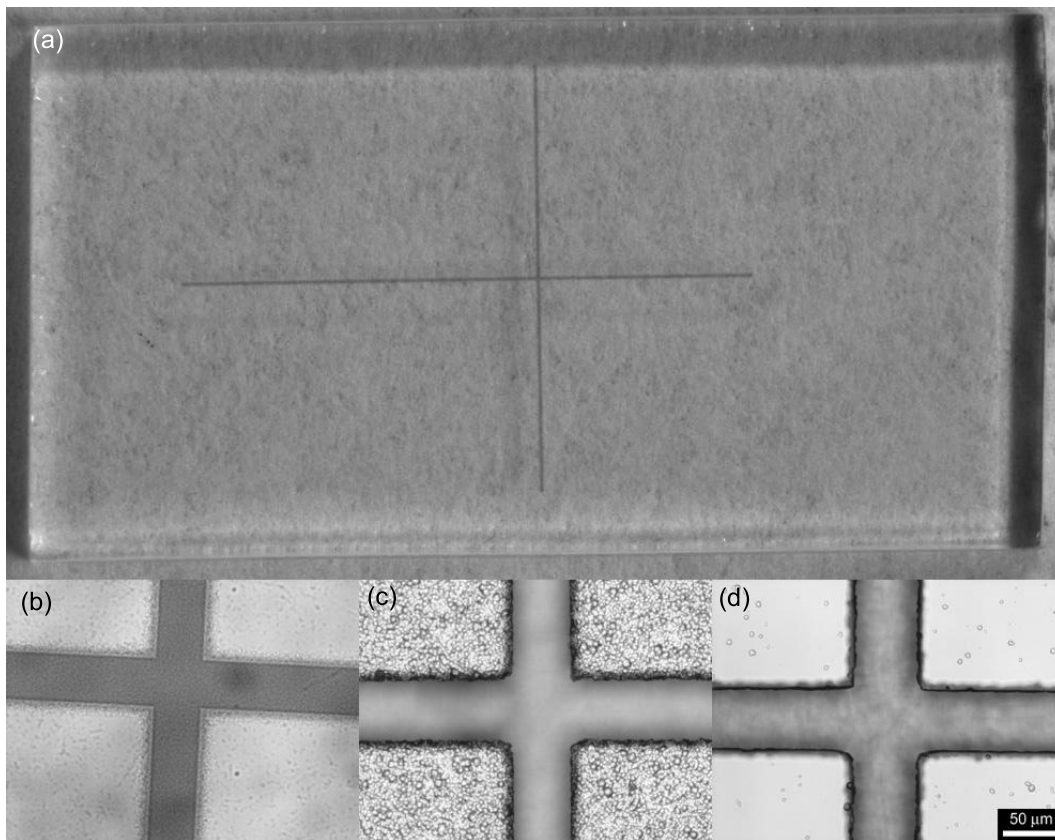

Figure 2. Optical images showing (a) Overview of the device, (b) the sample after heat treatment, (c) the sample after etching in HF, (d) the sample after polishing to remove the surface roughness.

Atomic Force Microscopy (AFM) was used to characterize the surface roughness before and after etching. The irradiated region, post heat treatment, had a surface root mean squared (RMS) roughness of between 6-10

nm. An AFM image of part of the irradiated region post annealing is shown in figure 3a. After etching in HF, the surface roughness increases dramatically. This can be seen in the AFM image of a region adjacent to the microchannel is shown in figure 3b. Pits appear on the surface of the sample that can be as high as several microns. Clearly, any induced surface roughness by the etching process will be transferred to the waveguide thus increasing the scattering loss. To overcome this problem, the surface of the sample was re-polished to achieve an optical finish before the integrated waveguides were fabricated. An image of the sample after polishing is shown in figure 2d. It has been also shown by Cheng et al[17] that the surface roughness may be reduced by a temperature annealing process. This method will be investigated in future studies.
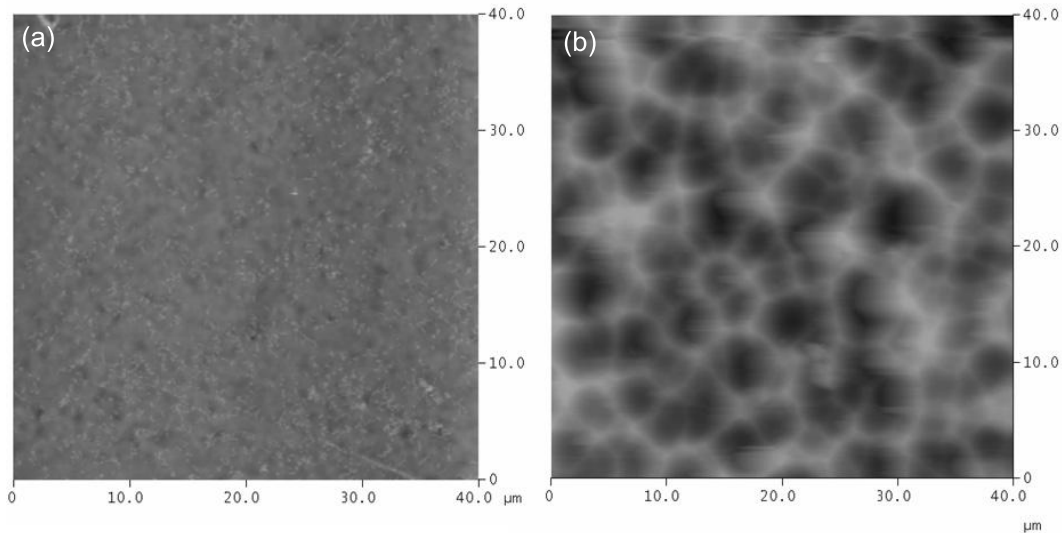

Figure 3. AFM images showing the sample before (a) and after (b) etching in HF.

2.2. Waveguide fabrication

Several waveguides were fabricated with fluences ranging between 1×10^{14} and 1×10^{16} protons/cm^2 in a second Foturan^{TM} sample using 2 MeV protons. This sample allowed us to independently test the waveguiding properties before fabricating the integrated waveguides in the microchannel sample. Optical characterization of the waveguides was performed using a 17 mW He-Ne (632.8 nm) laser that was launched into a single mode fiber (3M FS-SN3224). The fiber was butt-coupled to the end face of the waveguides and the emerging light was imaged using a 40× long working distance objective and a 12 bit cooled charge coupled device (CCD) camera (Qimaging Retiga Exi). The sample was placed on a 3-axis stage while input and output stages had 6-axes for precise control over the light coupling.

Propagation loss measurements were performed using the scattering technique.[18] Laser light was launched into the waveguides and the scattered light was imaged using a stereo zoom microscope mounted perpendicular to the waveguide. The loss values retrieved from the best fits were in the 8-13 dB/cm range, increasing with proton fluence. Figure 4 shows an image of the mode profile for a waveguide fabricated using 1×10^{16} protons/cm^2, and an optical image showing the edge view of the sample.

The integrated buried channel waveguides were fabricated using 1 MeV protons and a fluence of 1×10^{16} protons/cm^2. Although this fluence gave the highest value of propagation loss, it also gave the best mode profile. A reduced energy was used to fabricate the waveguide in order to position the end of range of the protons such that the waveguide core is located somewhere in the middle of the microchannel. In order to fabricate the waveguides the sample was scanned with the EXFO Burleigh inchworm stage at a speed of 2 μ/s with a perpendicular magnetic scan size of 8 μm. The waveguide was fabricated so that it crossed perpendicular to the microchannel, and over the two edges of the sample (See figure 1).
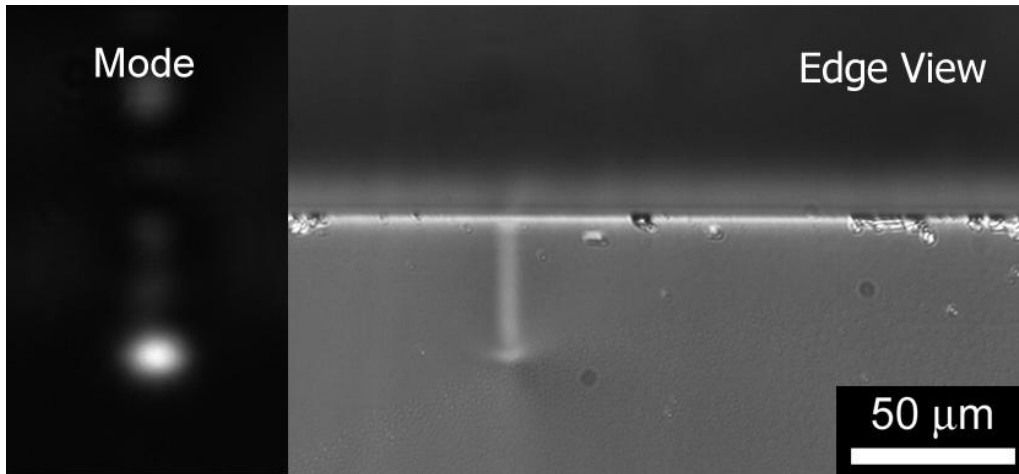
Figure 4. Optical image of the edge of a waveguide sample and a guided mode.

3. DISCUSSION

Foturan^{TM} glass is typically composed of 75-85% SiO_2 and 7-11% Li_2O along with 0.05-0.15% of Ag_2O and 0.02-0.04% of CeO_2.[6] The formation of lithium-metasilicate in Foturan^{TM} during heat treatment is the result of crystallization at Ag particles. The Ag occurs only in the irradiated region due to a reduction of the Ag^+ ions in the glass by the irradiation process. At 500°C Ag atoms begin to agglomerate to form larger Ag particles. Then as the temperture in increased to 600°C, Li_2SiO_2 crystallites ranging in size up to a few microns form around the Ag nuclei. If UV light is used to pattern Foturan^{TM}, the mechanism by which Ag^+ ions are reduced to Ag is the photo-oxidization of Ce^{3+} to the more stable Ce^{4+} ion. In this case Ce^{3+} is acting as a sensitizer by absorbing the UV photons and transferring an electron to the Ag^+ ions.

When an MeV proton impinges on a target it will penetrate into the sample loosing energy either by interacting with the target electrons (Electronic stopping) or by scattering off target nuclei (Nuclear stopping). The energy loss mechanism that dominates depends on the energy of the proton. Electronic energy loss occurs right through the proton range, peaking just before the end of range of the proton. Nuclear energy loss predominately occurs at the end of range. The electronic energy loss (Ionization) profile of 2 MeV protons in Foturan^{TM} is simulated using the Stopping and Range of Ions in Matter (SRIM) software package[19] and shown in figure 5. It can be seen from this profile that protons are able to cause the oxidization of Ce^{3+} throughout the range, resulting in a microchannel that is 45 μm in depth. This value will be reduced by the etching and polishing process.

For proton beam irradiation it is possible that in addition to this mechanism, other defects such as nonbonding oxygens (NBO) can take on the role of electron donor. These defects would predominantly occur towards the end of range in the nuclear stopping region. Hence both the proton electronic and nuclear energy loss process can play a role in the patterning of Foturan^{TM}.

PBW has been used previously to fabricate buried channel waveguides in a range of materials including polymers[20, 21] and glass.[22–24] The technique relies on the fact that the energetic protons impinging on the sample lose most of their energy when they slow down in the form of collisions with target electrons, and by introducing atomic displacements. This end of range energy deposition can result in either a compaction or swelling of material thus forming a region with altered refractive index which can be used for light guiding. Figure 5 shows the simulated vacancy profiles for 1 MeV and 2 MeV protons in Foturan^{TM} using SRIM. The waveguides fabricated using 1 MeV protons are predicted to be located approximately 15 μm below the surface. An optical image of the combined microchannel and waveguides is shown in figure 6.
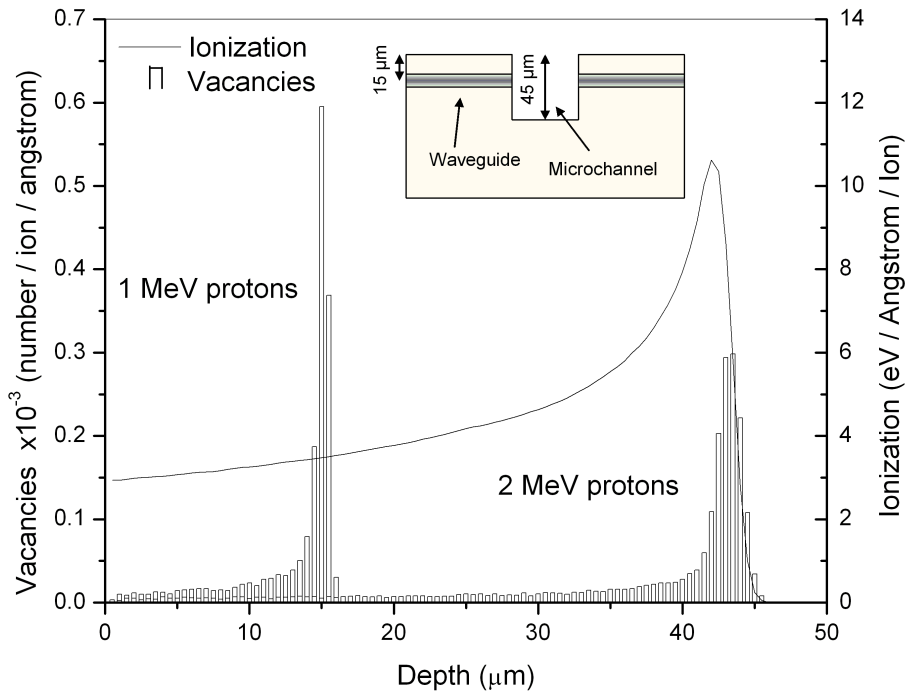
Figure 5. Simulated vacancy and ionization profiles for 1 MeV and 2 MeV protons in Foturan^{TM}. These results were simulated using the SRIM software package.
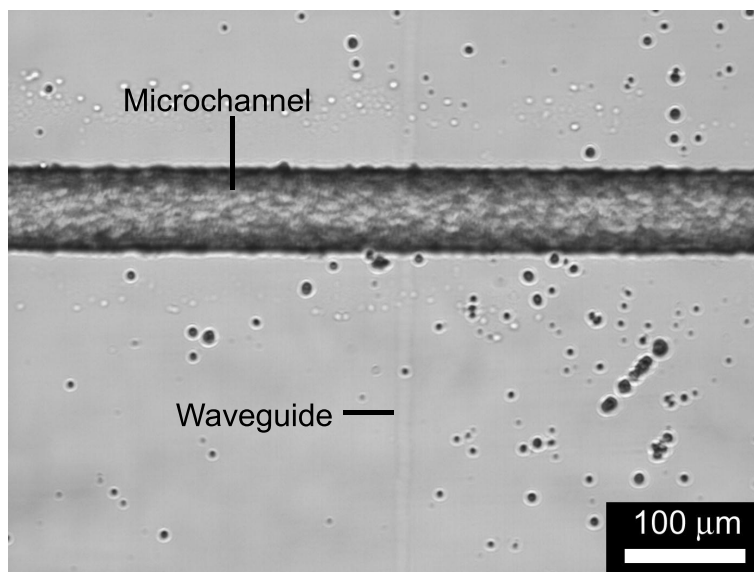

Figure 6. An optical image showing the final structure. The integrated waveguide can be seen crossing the microchannel.

4. CONCLUSION

In conclusion we have successfully fabricated a microchannel with an integrated waveguide in Foturan^{TM} photostructurable glass using the PBW technique. The structure was made using a multi step process that involved heat treatment and etching to form the channel, and a second irradiation step in order to fabricate the buried waveguide. Future work will concentrate on improving the surface roughness of the channel and optically characterizing the the integrated waveguide structure. In principal, the same procedure can be used to make similar structures in polymers like PMMA. Any number of microchannels and waveguides buried at various depths can be made using this method. PBW can also be used to build up more complicated biophotonic lab-on-a-chip devices with integrated optics.

REFERENCES

1. D. A. Cohen, J. Nolde, C. Wang, E. Skogen, A. Rivlin, and L. Coldren, "Biophotonic integrated circuits," *Proceedings of SPIE* **5594**, pp. 81–93, 2004.
2. H. Qiao, S. Goel, A. Grundmann, and J. McMullin, "Biochips with integrated optics and fluidics," *Proceedings of SPIE* **5062**, pp. 873–878, 2002.
3. S. Goel, H. Qiao, A. Grundmann, and J. McMullin, "Fabrication of micro-optic/microfluidic biochips," *Proceedings of SPIE* **4833**, pp. 54–59, 2002.
4. Y. Cheng, K. Sugioka, K. Midorikawa, M. Masuda, K. Toyoda, M. Kawachi, and K. Shihoyama, "Control of the cross-sectional shape of a hollow microchannel embedded in photostructurable glass by use of a femtosecond laser," *Opt. Lett.* **28**, p. 55, 2003.
5. F. Watt, J. van Kan, and T. Osipowicz, "Three-dimensional micro fabrication using mask less irradiation with mev ion beams: proton beam micromachining," *MRS Bulletin* **25**, pp. 33–38, 2000.
6. T. R. Dietrich, W. Ehrfeld, M. Lacher, M. Kramer, and B. Speit, "Fabrication technologies for microsystems utilizing photoetchable glass," *Microelec. Eng.* **30**, pp. 497–504, 1996.
7. M. Masuda, K. Sugioka, Y. Cheng, N. Aoki, M. Kawachi, K. Shihoyama, K. Toyoda, H. Helvajian, and K. Midorikawa, "3d microstructuring inside photosensitive glass by femtosecond laser excitation," *Appl. Phys. A* **76**, pp. 857–860, 2003.
8. J. Kim, H. Berberoglu, and X. Xu, "Fabrication of microstructures in photoetchable glass ceramics using excimer and femtosecond lasers," *J. Microlith. Microfab. Microsyst.* **3**, pp. 478–485, 2004.
9. S. Juodkazis, K. Yamasaki, V. Mizeikis, S. Matsuo, and H. Misawa, "Formation of embedded patterns in glasses using femtosecond irradiation," *Appl. Phys. A* **79**, pp. 1549–1553, 2004.
10. M. Abraham, I. Gomez-Morilla, M. Marsh, and G. Grime, "Proton induced structuring of a photostructurable glass," *Mat. Res. Soc. Proc* **739**, p. H2.8.1, 2003.
11. I. Rajta, I. Gomez-Morilla, M. H. Abraham, and A. Z. Kiss, "Proton beam micromachining on pmma, foturan and cr-39 materials," *Nucl. Instr. Meth. B* **210**, pp. 260–265, 2003.
12. I. Gomez-Morilla, M. H. Abraham, D. G. de Kerckhove, and G. W. Grime, "Micropatterning of foturan photosensitive glass following exposure to mev proton beams," *J. Micromech. Microeng.* **15**, pp. 706–709, 2005.
13. A. C. Fisher, K. A. Gooch, I. E. Henley, and K. Yunus, "Voltammetry under microfluidic control," *Analytical Sci.* **17**, p. i371, 2001.
14. K. Sugioka, Y. Cheng, and K. Midorikawa, "3D micromachining of photosensitive glass by femtosecond laser for microreactor manufacture," *Journal of Photopolymer Science And Technology* **17**, pp. 397–402, 2004.
15. V. R. Bhardwaj, E. Simova, P. B. Corkum, D. M. Rayner, C. Hnatovsky, R. S. Taylor, B. Schreder, M. Kluge, and J. Zimmer, "Femtosecond laser-induced refractive index modification in multicomponent glasses," *Jour. Appl. Phys.* **97**, p. 083102, 2005.

16. Y. Cheng, K. Sugioka, M. Masuda, K. Shihoyama, K. Toyoda, and K. Midorikawa, "Optical gratings embedded in photosensitive glass by photochemical reaction using a femtosecond laser," *Optics Express* **11**, pp. 1809–1816, 2003.

17. Y. Cheng, K. Sugioka, K. Midorikawa, M. Masuda, K. Toyoda, M. Kawachi, and K. Shihoyama, "Three dimensional micro-optical components embedded in photosensitive glass by a femtosecond laser," *Opt. Lett.* **28**, p. 1144, 2003.

18. S. V. Rao, K. Moutzouris, M. Ebrahimzadeh, A. D. Rossi, M. Calligaro, V. Ortiz, G. Ginitz, and V. Berger, "Measurements of optical loss in gaas/al2o3 nonlinear waveguides in the infrared using femtosecond scattering technique," *Opt. Commun.* **213**, p. 223, 2002.

19. J. F. Ziegler, "Srim 2003," *Nucl. Instrum. Meth. B* **219-220**, p. 1027, 2004.

20. T. C. Sum, A. A. Bettiol, J. A. van Kan, F. Watt, E. Y. B. Pun, and K. K. Tung, "Proton beam writing of low loss polymer optical waveguides," *Appl. Phys. Lett.* **83**, p. 1707, 2003.

21. T. C. Sum, A. A. Bettiol, H. L. Seng, I. Rajta, J. A. van Kan, and F. Watt, "Proton beam writing of passive waveguides in pmma," *Nucl. Instrum. Meth. B* **210**, p. 266, 2003.

22. A. Roberts and M. von Bibra, "Fabrication of buried channel waveguides in fused silica using focused mev proton beam irradiation," *J. Lightwave Tech* **14**, pp. 2554–2557, 1996.

23. M. von Bibra and A. Roberts, "Refractive index reconstruction of graded index buried channel waveguides from their mode intensities," *J. Lightwave Tech* **15**, pp. 1695–1699, 1997.

24. K. Liu, E. Y. B. Pun, T. C. Sum, A. A. Bettiol, J. A. van Kan, and F. Watt, "Erbium doped waveguide amplifiers fabricated using focused proton beam direct-writing," *Appl. Phys. Lett* **84**, p. 684, 2004.